Available online at www.sciencedirect.com
ScienceDirect
Microelectronic Engineering 85 (2008) 886–889
MICROELECTRONIC ENGINEERING
www.elsevier.com/locate/mee

Fabrication of photonic components by nanoimprint technology within ePIXnet

U. Plachetka [a,*], A. Kristensen [b], S. Scheerlinck [c], J. Huskens [d], N. Koo [a], H. Kurz [a]

[a] *Advanced Microelectronic Centre Aachen (AMICA), 52074 Aachen, Germany*
[b] *MIC Department of Micro and Nanotechnology, 2800 Kongens Lyngby, Denmark*
[c] *Ghent University-IMEC, Department of Information Technology, 9000 Ghent, Belgium*
[d] *MESA+ Institute for Nanotechnology, University of Twente, 7500 AE Enschede, Netherlands*

Received 5 October 2007; received in revised form 14 December 2007; accepted 10 January 2008
Available online 18 January 2008

Abstract

The joined research activities on nanoimprint lithography (JRA-NIL) within a European Network of Excellence (ePIXnet) are described. The achievements are presented in three different exemplary applications.

Keywords: Nanoimprint; Photonics; ePIXnet; Nanoparticles

1. Introduction

The "*European Network of Excellence on Photonic Integrated Components and Circuits*" (ePIXnet) has been developed to an efficient platform where research facilities are integrated. Industry and academics perform joint research activities in the field of integrated photonics. The integration of complex or high performance photonic functions will become the key enabler for a cost-effective and ubiquitous deployment of photonics in a wide range of applications, including ICT-applications, sensor applications and medical applications. Here, the joint research activity nanoimprint lithography (JRA-NIL) within ePIXnet is devoted to investigate the potential of nanoimprint as a fabrication technique for photonic devices. The three main advantages of nanoimprint are the comparatively low tool costs, the high resolution in the sub-10 nm regime and the capability to replicate a given 3D-topography. In this paper three exemplary application fields are detailed and the potentials in developments for passive silicon resonators, a hybrid imprint fabrication process for polymeric DFB-Lasers and the assembly of nanoparticles (NPs) on functionalised imprint patterns are explored.

2. Fabrication of silicon ring resonator

In the JRA-NIL a number of photonic patterns from waveguides, delay guides, couplers, splitters, mach-zehnder to photonic crystals have been patterned by nanoimprint. An element that is often used to qualify a fabrication process for silicon photonic devices is the microring resonator in silicon waveguide technology. Typical SOI ring resonators, fabricated mostly by electron beam lithography (EBL) or deep UV lithography (DUV), have radii between 3 μm and 20 μm, waveguide width between 250 nm and 500 nm and coupling distances ranging from 70 nm (only EBL) to 400 nm. Here depending on the fabrication procedures and used device dimensions propagation losses between 350 dB/cm down to 1.9 dB/cm and quality factors in silicon between 1000 and 139,000 have been realized [1].

In JRA-NIL microring resonators with a radius of 10 μm, waveguide width of 465 nm and a coupling distance of 243 nm were patterned using a soft UV-nanoimprint lithography process (soft UV-NIL) [2]. In soft UV-NIL the flexible imprint template is fabricated using a cast moulding

* Corresponding author. Tel.: +49 241 8867 202; fax: +49 241 8867 571.
E-mail address: plachetka@amo.de (U. Plachetka).

0167-9317/$ - see front matter © 2008 Elsevier B.V. All rights reserved.
doi:10.1016/j.mee.2008.01.013

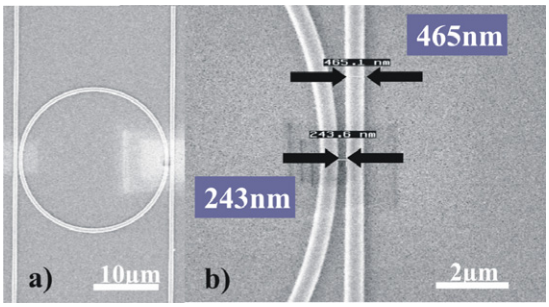

Fig. 1. (a) Imprinted microring resonator and (b) close-up of 243 nm gap between ring and 465 nm broad waveguide.

process. Here a polymer (i.e. PDMS) is poured onto a silicon master, and cured by thermal treatment on a hotplate. This cured polymer layer is then used in the imprint process. Due to its flexible nature the polymeric template can easily compensate for surface waviness of a given substrate making it possible to imprint with pressures below 100 mbar [3]. The soft UV-NIL process is then carried out as follows; first a thin layer of a UV-curable low molecular resist is spin-coated on a SOI-substrate, then the flexible imprint template is pressed into the liquid resist with a pressure of 50 mbar after which the resist is cured directly through the transparent template by UV-light. In a last process step the imprint template is detached from the patterned SOI substrate and may be used for subsequent imprint steps. Thus the cured resist layer on the SOI resembles the faithful negative counterpart of the used PDMS imprint template.

After the resist patterning on the SOI a plasma etching process for transferring the microring resonator into the 310 nm top silicon follows. Here first the residual imprint resist layer is removed in a BCl_3-plasma, followed by two step etching process mainly using HBr plasma into the top silicon layer down to the BOX. In Fig. 1a the imprinted microring resonator is shown; the close-up in Fig. 1b details the gap on the right side of the resonator. Fig. 2.

Optical characterization of the fabricated SOI microring resonators was carried out using a commercial transmission characterization system comprising a wavelength-tunable external cavity diode laser and a photodiode. Fig. 3 details the spectral response measured at the through (upper solid line) and drop (lower solid line) channel of the waveguides exhibiting the expected resonant intensity modulation. To determine the corresponding quality factor Q, the experimental data were numerically fitted by an analytical transfer function [4]. The quality factor was measured to $Q = 47{,}000$ with propagation losses of 3.5 dB/cm.

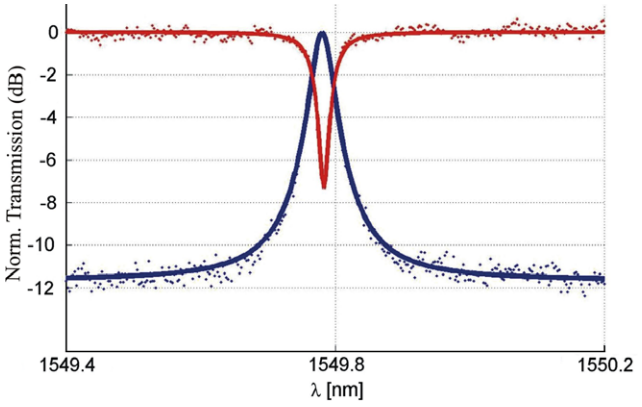

Fig. 2. Spectral response measured at the through (upper solid line) and the drop (lower solid line) channel showing resonant intensity modulation.

3. Hybrid imprinting of polymer DFB-laser

In addition to the approach to replicate a 3D-template via imprinting, other methods can be combined with nanoimprint to obtain 3D structures in one lithography step. One such method based on the combination of high resolution UV-NIL and optical lithography is explored by fabricating specific structures for dye lasers. The combined nanoimprint and photolithography (CNP) relies on a transparent imprint template with nm sized protrusions and an integrated shadow mask for µm sized structures [5]. The CNP process is shown in Fig. 3a; in Fig. 3b the schematic assembly of the device can be seen. SU-8 doped with rhodamine 6G is spin coated onto a silicon wafer with 3 µm thermal oxide on its surface [6]. Then the hybrid CNP

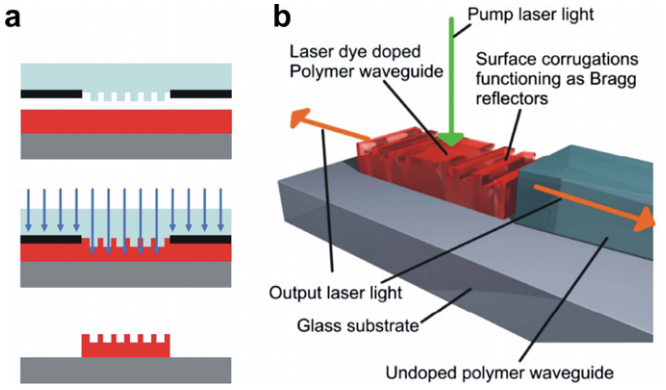

Fig. 3. (a) CNP process flow; (b) schematic assembly of polymer DFB-Laser.

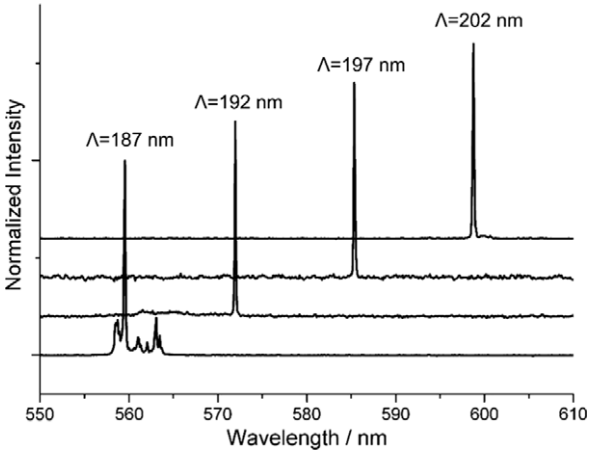

Fig. 4. Spectra from four DFB lasers pumped at 39 µJ/mm^2; the emission wavelength depends on the grating period.

Table 1
Measured data on wavelength (λ) and threshold pump fluences Qth for functional devices from a 4 inch wafer

Pitch A (nm)	λ_{Design} (nm)	n_{eff} @ λ_{Design}	λ_0 (nm)	$\sigma(\lambda_0)$ (nm)	Q_{th} (μJ/mm^2)	$\sigma(Q_{th})$(μJ/mm^2)
187	556	1.486	559.2	1.6	14.6	2.0
190	570	1.485	571.3	0.9	17.0	3.6
200	584	1.483	585.9	0.8	13.0	2.9
205	598	1.481	599.7	0.8	10.4	2.3

imprint template is pressed into the polymer at 100 °C with an imprint pressure of 12.7 bar. After UV-exposure and post exposure bake the CNP-template is removed from the substrate and the SU-8 is developed in PGMEA leaving behind a free standing functionalized resist body with μm–mm dimensions and a high resolution DFB grating on top.

Measurements were performed connecting the laser via waveguide and polymeric fiber to a fixed grating spectrometer. Here a number of DFB-lasers were build with slight shifts in the grating period on the top of the device.

In Fig. 4 the dependency of the output wavelength on the grating period of four lasers is shown.

In Table 1 the numerical data on the emission wavelength (λ_0) and laser threshold fluences (Q_{th}) are given. Measurements show that the emission wavelength (λ_0) is within ±2 nm of the calculated design wavelength (λ_{Design}) for the fabricated pitch.

4. Assembly of NPs on imprinted surfaces by noncovalent interactions

Being able to place nano-objects at the desired position is of highest interest for the possible integration of these building blocks into devices [7]. Among these nano-objects, nanoparticles (NPs) are one of the most widespread. Integration of NPs with high accuracy inside circuits is a promising route for the development of photonic devices, high-density patterned media, and catalysis [8]. When the surface of the referred nanoparticles is functionalized, they have a potential as chemical and biological sensors [9]. One type of interaction that has been used for attachment of NPs is the supramolecular one, using host-guest chemistry. Here cyclodextrin (CD) monolayers as so-called molecular printboards were used, i.e., as substrates onto which (bio)molecules, supramolecular assemblies, and nanoparticles can be immobilized using specific, noncovalent interactions. Adamantyl-functionalized dendrimers, which can function as a supramolecular glue for the aggregation of CD-functionalized gold nanoparticles in solution, provide the attachment of CD-functionalized gold and silica nanoparticles onto the CD molecular printboards. The spherical nature of both dendrimers and nanoparticles, after their respective adsorptions resulting in surfaces exposing guest and host groups, provides a route to incorporate these adsorption processes into a layer-by-layer assembly scheme (Fig. 5) [10].

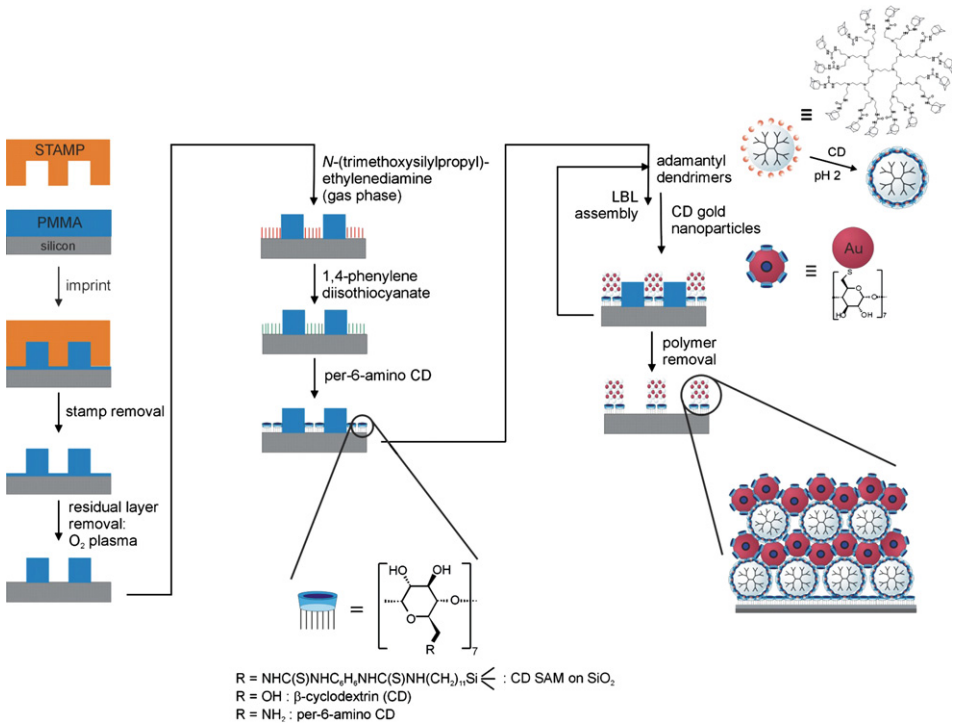

Fig. 5. Integrated nanofabrication scheme on nanoimprinted pattern, self-assembled monolayer formation (left) and layer-by-layer assembly (right).

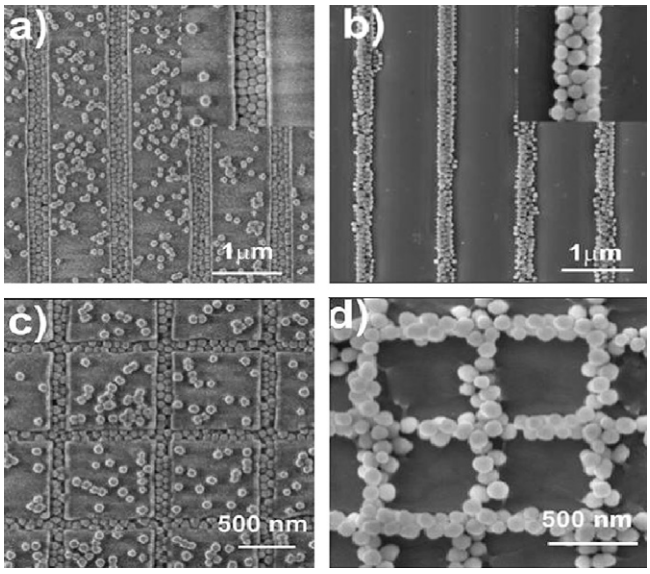

Fig. 6. SEM images of CD layer patterns in the form of (a, b) 200 nm wide lines, (c, d) 150 nm wide grids, after (a, c) one bilayer formation and (b, d) 2 bilayers formation.

This approach appeared to be fully compatible with the presence of NIL-prepared PMMA structured substrates. NIL-patterned CD monolayers were made, and used as templates for the directed assembly of CD-functionalized gold and silica NPs (Fig. 6), also in layer-by-layer assembly schemes. Essential in this layer-by-layer assembly method is that possible nonspecific adsorption, which does occur in the case of directed LBL assembly on patterned SAMs, of these components onto the PMMA structures does not pose any problems because the polymer is dissolved in the final lift-off step together with the material deposited onto it, analogous to the use of NIL-prepared PMMA structures for metal evaporation and lift-off. In such an integrated process, supramolecular multilayer hybrid nanostructures down to 50 nm lateral size and 20 nm height have been prepared [11].

5. Conclusion

The main emphasis of the JRA-NIL in ePIXnet is the implementation of nanoimprint as a low cost and adaptive lithography method for photonic components. Thus passive photonic devices in silicon waveguide technology have been fabricated with quite acceptable results in comparison with other lithography methods. Yet, nanoimprint can be used beyond standard patterning. It can be combined with other techniques in so called hybrid lithography processes to broaden the spectrum of application areas. These process variations may go hand in hand in the use of dedicated functionalized resists which make etching processes obsolete. In this respect the integration or formation of nano-objects on imprinted pattern poses one of the most interesting process extensions. Ultimately the integration of these processes can lead to enhanced and novel photonic devices.

Acknowledgements

This work is partially supported by the European Community under the NaPa Contract No. NMP4-CT-2003-500120, Circles of Light Contract No. FP6-034883, and the network of excellence ePIXnet. The work of M. Först, M. Waldow and M. Gersborg-Hansen is highly appreciated.

References

[1] J. Niehusmann, A. Vörckel, P. Haring Bolivar, T. Wahlbrink, W. Henschel, H. Kurz, Opt. Lett. 29 (2004) 2861–2863.
[2] U. Plachetka, M. Bender, A. Fuchs, B. Vratzov, H. Kurz, Microelectron. Eng. 73–74 (2004) 167–171.
[3] U. Plachetka, M. Bender, A. Fuchs, T. Wahlbrink, T. Glinsner, H. Kurz, Microelectron. Eng. 83 (2006) 944–947.
[4] Vörckel, M. Mönster, W. Henschel, P. Haring Bolivar, H. Kurz, IEEE Photon. Technol. Lett. 15 (2003) 921–923.
[5] M. Christiansen, M. Scholer, A. Kristensen, Opt. Express 15 (7) (2007) 3931–3939.
[6] D. Nilsson, S. Balslev, M.M. Gregersen, A. Krsitensen, Appl. Opt. 44 (2005) 4965–4971.
[7] G.A. Ozin, I. Manners, S. Fournier-Bidoz, A. Arsenault, Adv. Mater. 17 (2005) 3011–3018.
[8] M. Antonietti, G.A. Ozin, Chem. Eur. J. 10 (2004) 28–41.
[9] A.N. Shipway, E. Katz, I. Willner, Chem. Phys. Chem. 1 (2000) 18–52.
[10] O. Crespo-Biel, B. Dordi, D.N. Reinhoudt, J. Huskens, J. Am. Chem. Soc. 127 (2005) 7594–7600.
[11] P. Maury, M. Péter, O. Crespo-Biel, X.Y. Ling, D.N. Reinhoudt, J. Huskens, Nanotechnology 18 (2007) 044007.